

13.1;06.5

The features of the surface morphology of thin conductive films of indium-tin oxides obtained by laser-oriented deposition

© A.S. Toikka^{1,2}, N.V. Kamanina^{1–3}

¹ St. Petersburg State Electrotechnical University, „LETI“, St. Petersburg, Russia

² St. Petersburg Institute of Nuclear Physics named after. B. P. Konstantinov

Research and Engineering Center „St. Petersburg Nuclear Physics Institute, National Research Center Kurchatov Institute, Gatchina, Russia

³ JSC „Scientific and Production Association State Optical Association S.I. Vavilov Institute“

JSC „State Optical Institute S.I.Vavilov“, Saint-Petersburg, Russia

E-mail: atoikka@obraz.pro

Received September 8, 2023

Revised October 30, 2023

Accepted November 1, 2023

The effect of the control electric field strength on the surface properties of laser-deposited thin films based on indium tin oxides (ITO) has been studied. It is shown that with increasing control field strength, the roughness of coatings decreases from 3.4 to 0.4 nm. When wetting with drops of distilled water, it was found that at $E = 0$ V/cm the Cassie–Baxter state is realized, at field $E = 100$ V/cm a transition to the Wenzel state is observed, and with a further increase in the electric field strength, dynamics appears in the direction towards the ideally smooth surface model.

Keywords: laser-oriented deposition, indium tin oxides, transparent conductive contacts.

DOI: 10.61011/0000000000

Indium tin oxide (ITO) — a degenerate semiconductor with n -type conduction. Due to their spectral properties, relatively affordable technology for varying the stoichiometric composition, and low electrical resistivity, ITO-based thin films serve as transparent contacts in modulation and display technology, solar cells, and sensors [1–4]. The surface properties of ITO can be significantly tunable [5,6], which also allows us to consider this material as substrates for microfluidics and spin-coating [7] of functional layers. The scientific and practical problem of developing ITO coatings is related to the search for deposition and processing methods that allow this material to be adapted to an extensive list of specified applications. Magnetron and thermal spraying are used for mass production, but the ITO surface is relatively rough [8] and there is a large loss of material. Atomic layer deposition produces more homogeneous coatings [9], but the scale of production is limited by the high cost of equipment. Separately, we will single out laser deposition methods [10,11], in which the flow of deposited particles is controlled by means of optical parameters. Moreover, the vacuum post is mechanically separated from the optical circuitry, which is a significant advantage in plant maintenance. When considering the method of laser-oriented deposition [11], it is necessary to emphasize the possibility of additional orientation of the deposited particles by means of an electric field, the use of a wide range of matrix materials, deposited particles and used substrates [12,13]. Also in the case of laser-directed ITO deposition, additional surface treatment by direct laser

ablation and surface electromagnetic wave [14] treatment is available.

The present work is devoted to the possibility of reshaping the surface topography of ITO films by varying the controlling electric field during their deposition. This approach is due to the dramatic change in wetting mechanisms when varying deposition regimes. Groups of ITO thin film samples with thicknesses in the range of 95–108 nm and RMS roughness to 3.4 ± 1.1 nm that were deposited in the absence of a controlling electric field ($E = 0$ V/cm) and at field strengths of 100, 200, and 600 V/cm were compared. An CO₂ laser ($\lambda = 10.6 \mu\text{m}$) with an operating power of 30 W, a beam diameter of 5 mm, and a processing speed of 3 cm/s was used for all deposited structures. The source of ITO was Cerac Inc. brand pellets. ((In₂O₃)_{0.9}–(SnO₂)_{0.1}, 99.99%, dispersity 3–12 μm). The thin films were deposited on substrates based on crown K8 optical glass. Scanning electron microscope „FEI Quanta“ (working pressure 10^{-4} Pa, accelerating voltage 1 kV), atomic force microscope (AFM) „Solver Next NT-MDT“ (contact mode, scanning frequency 1 Hz, scan area $10 \times 10 \mu\text{m}$), OCA 15EC DataPhysics contact wetting angle measurement system (lying drop method, test liquid — distilled water with polar and dispersion components of surface tension 48.1 and 24.1 mN/m), J.A. Woolam M-2000RCE ellipsometer (reflectometry mode, averaging over 26 points within the aperture).

According to scanning electron microscopy (SEM) data, for all the mentioned regimes the surface of laser-deposited ITO films is granular with characteristic gaps (Fig. 1).

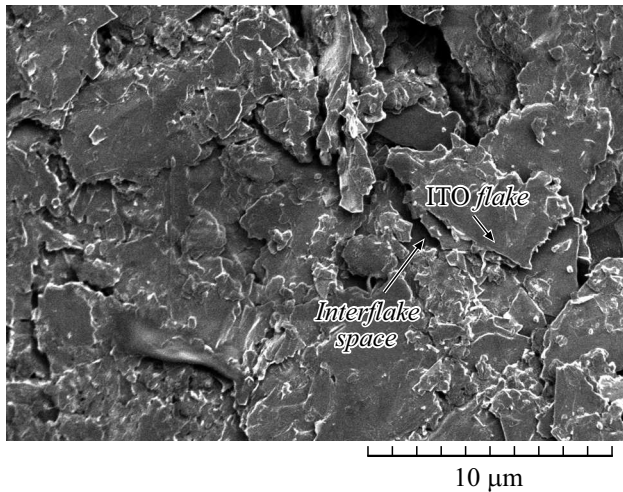


Figure 1. SEM image of the surface of ITO film obtained by laser-oriented deposition.

Analysis of AFM scans of ITO surfaces indicates that the arithmetic mean surface roughness (E) decreases with increasing electric field strength (S_a) during ITO deposition. At no field $S_a = 3.4 \pm 1.1$ nm, at $E = 100$ V/cm $S_a = 1.6 \pm 0.4$ nm, at subsequent increase in strength $S_a = 0.6 \pm 0.2$ nm ($E = 200$ V/cm) and $\Delta S_a = 0.4 \pm 0.3$ nm ($E = 600$ V/cm). The differences in surface topography of ITO films deposited under different conditions are clearly shown by comparing the contact wetting angle (θ_{CB}), which is generally defined as follows [15]:

$$\cos \theta_{CB} = rf \cos \theta_Y + (f - 1). \quad (1)$$

The θ_{CB} value corresponds to the contact angle for the Cassie–Baxter state, in which the parameter f — the fraction of the interface area of the solid – liquid. The parameter r corresponds to the ratio of the surface area in contact with the droplet to the cross-sectional area of the droplet in the contact plane. At $f = 1$, Baxter’s – Cassie state transitions to the Wenzel state. At $r = 1$, the Wenzel condition transitions to a perfectly smooth surface model, an equilibrium wetting angle (θ_Y) is observed that depends on the free surface energy (γ_s^p, γ_s^d) and surface tension (γ_l^p, γ_l^d) [15]:

$$\frac{(\gamma_l^p + \gamma_l^d)(1 + \cos \theta_Y)}{2\sqrt{\gamma_l^d}} = \sqrt{\gamma_s^p} \sqrt{\frac{\gamma_l^p}{\gamma_l^d}} + \sqrt{\gamma_s^d}. \quad (2)$$

The p index corresponds to polar components and the d index — dispersive components. The [16] shows a variation of γ_s within 16–24 mJ/m², which corresponds to $\theta_{CB} = 98$ –110°. ITO has also been reported to have pronounced hydrophilic properties ($\theta_{CB} = 64^\circ$) [17].

Thus, the free surface energy components of ITO, which are features of the material itself, are highly dependent on the substrate material, deposition methods and subsequent processing. Consequently, there appears to be no fixed

theoretical value of θ_Y for ITO. Statistical data on the wetting of laser-deposited ITO films by distilled water droplets are presented in Fig. 2.

Based on the comparative data, it can be stated that in the absence of electric field during ITO deposition, the surface is hydrophobic. This corresponds to $\theta_Y \approx 92$ – 95° , $3 < r < 5$ and $0.6 < f < 0.9$ (Baxter’s–Cassie state). At $E = 100$ V/cm, the ITO surface is also relatively rough, but insufficient to form a stable air gap between the heterogeneities. From the comparison of the experimental data with the analytical calculation, it follows that $\theta_Y \approx 85$ – 87° , $2.5 < r < 4.5$ and $0.9 < f < 1$ (a state close to the Wenzel state). The ITO surfaces corresponding to the deposition conditions of $E = 200$ and 600 V/cm have relatively low roughness. Therefore, when considering the wetting phenomenon, it is possible to perceive these states as close to the model of perfectly smooth surfaces. However, Fig. 2 shows that these conditions are characterized by significant fluctuations in the contact wetting angle. From the analysis of expression (1), it follows that θ_Y corresponds to the boundary condition between hydrophilic and hydrophobic.

The influence of the electric field in the ITO deposition process is also evident in the refractive properties of the thin film surfaces. As the electric field strength increases, the reflection coefficient increases (Fig. 3). This result can be explained by a decrease in the number of air gaps on the ITO surface and a corresponding increase in the packing density. Since the refractive index of ITO is higher than that of air, more light is reflected within the aperture of the optical beam. At the same time, it should be taken into account that Fig. 3 presents data for polarized components, which characterizes the specular reflection (R_ϕ) to a greater extent. Since ITO films have inhomogeneities within the optical beam aperture, these structures are also characterized by the presence of diffuse reflection (R_d). Therefore, the increase in the reflection coefficient in Fig. 3 can be explained by the change in the ratio R_ϕ/R_d .

Thus, based on the available experimental data and theoretical assumptions, the following aspects should be highlighted. The surface roughness of ITO thin films decreases with the increase of the control electric field in the range of 0–600 V/cm in the process of laser-oriented deposition. In the absence of a control field, Baxter’s Cassi–state is realized. Since the equilibrium wetting angle exceeds 90° ($\theta_Y \approx 92$ – 95°), the subsequent increase in roughness r results in an increase in θ_{CB} (cm. (1)). In particular, roughness growth can be achieved by laser ablation or etching. From a practical point of view, this effect finds application in moisture-resistant optics. With $E = 100$ V/cm, the Wenzel condition of water wetting is realized in the deposition process. The equilibrium wetting angle at this regime is smaller than 90° ($\theta_Y \approx 85$ – 87°), so according (1), the subsequent increase in roughness r leads to a decrease in θ_{CB} . This effect is applicable to the development of microfluidic chips as well as the use of ITO as substrates for subsequent centrifugation

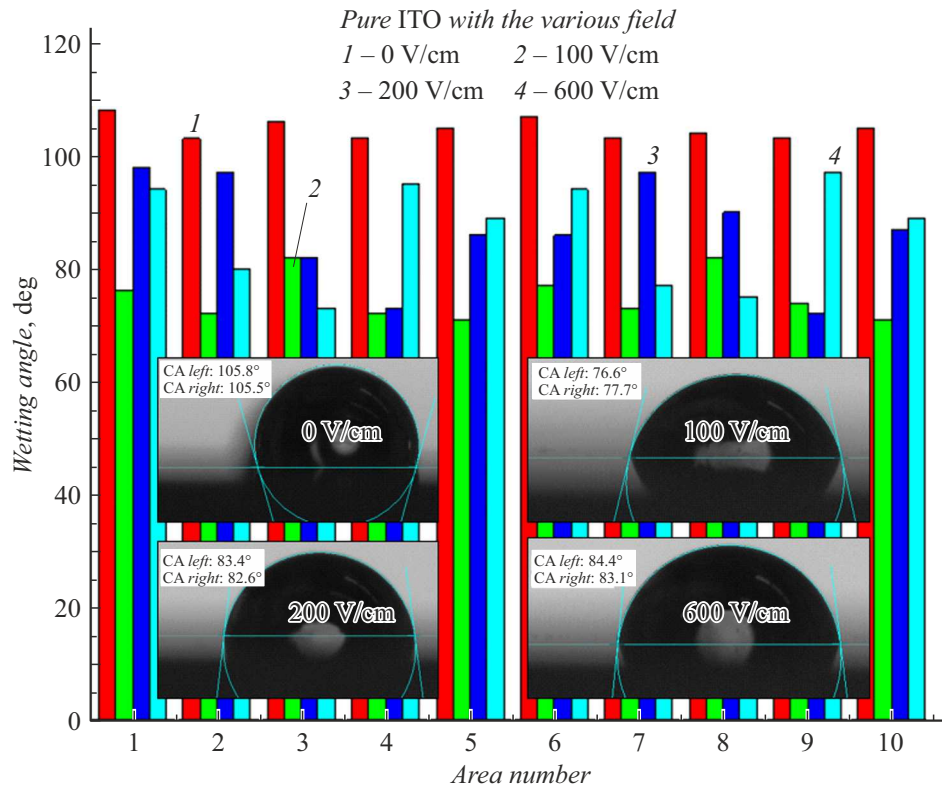


Figure 2. Statistics of contact wetting angles and examples of wetting of ITO film surfaces deposited at different electric field strengths.

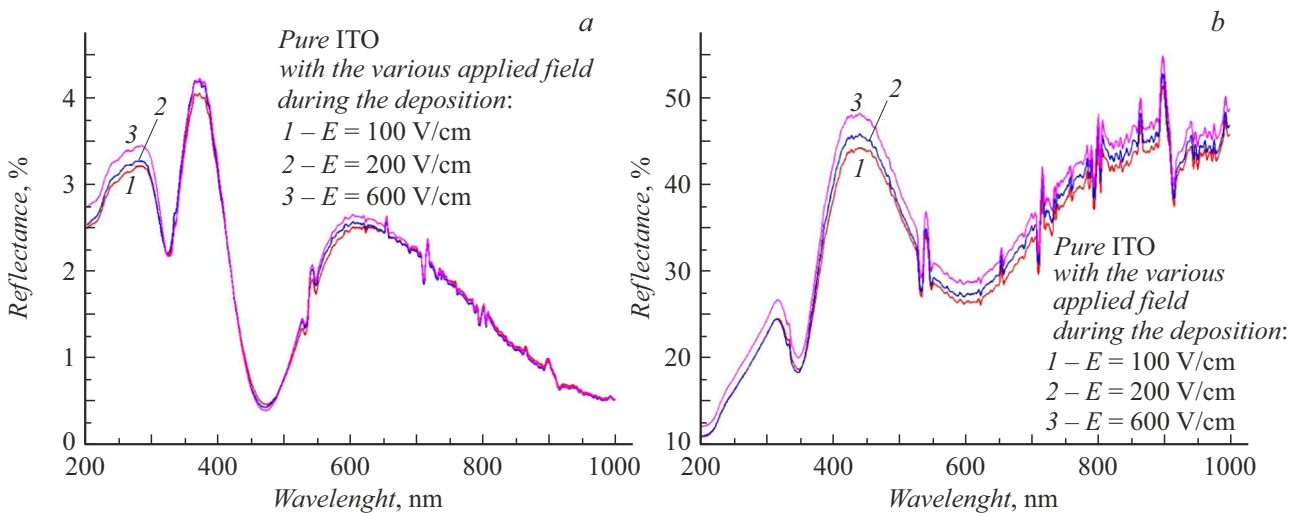


Figure 3. Comparison of the reflection coefficient of ITO thin films deposited under different electric field strengths (angle of incidence 65° with respect to the normal). *a* — *p* polarization, *b* — *s*-polarization.

of functional layers. Samples deposited at electric field strengths of 200 and 600 V/cm have relatively small roughness. It is difficult to use these configurations in their original form for wetting-related tasks, as they alternately exhibit hydrophilic and hydrophobic properties in different domains. However, from the reduced roughness and from the reflectance spectral dependencies, it is evident that a reduced porosity of ITO films is observed under these deposition conditions. Consequently, it is reasonable

to use these modifications as starting materials for the subsequent deposition of nanostructures. The described changes in the wetting mechanisms of ITO films can be interpreted as a way to adapt the surface to liquids with different surface tension. Thus, the control field strength is an additional parameter in the development of hydrophobic (for moisture-resistant optics), orienting (for liquid crystal devices) and hydrophilic (for microfluidics and centrifugation applications) coatings.

Conflict of interest

The authors declare that they have no conflict of interest.

References

- [1] S. Rajput, V. Kaushik, S. Jain, P. Tiwari, A.K. Srivastava, M. Kumar, *J. Lightwave Technol.*, **38** (6), 1365 (2019). DOI: 10.1109/JLT.2019.2953690
- [2] N.V. Kamanina, Yu.A. Zubtsova, A.S. Toikka, S. Likhomanova, A. Zak, R. Tenne, *Liq. Cryst. and their Appl.*, **20** (1), 34 (2020). DOI: 10.18083/LCAppl.2020.1.34
- [3] J.H. Kim, H.J. Seok, H.J. Seo, T.Y. Seong, J.H. Heo, S.H. Lim, K.J. Ahn, H.K. Kim, *Nanoscale*, **10** (44), 20587 (2018). DOI: 10.1039/C8NR06586A
- [4] M. Śmietana, M. Koba, P. Sezemsky, K. Szot-Karpińska, D. Burnat, V. Stranak, J. Niedziółka-Jönsson, R. Bogdanowicz, *Biosensors Bioelectron.*, **154**, 112050 (2020). DOI: 10.1016/j.bios.2020.112050
- [5] N.V. Kamanina, A.A. Kukharchik, P.V. Kuzhakov, Yu.A. Zubtsova, R.O. Stepanov, N.V. Baryshnikov, *Liq. Cryst. and their Appl.*, **15** (3), 109 (2015). DOI: 10.18083/LCAppl.2015.3.109
- [6] M. Musztyfaga-Staszuk, K. Gawlińska-Necek, R. Socha, P. Panek, *Materials*, **16** (4), 1363 (2023). DOI: 10.3390/ma16041363
- [7] M. Das, M. Kohlstädt, M. Enders, S. Burger, H.S. Sasmal, B. Zimmermann, A. Schäfer, B.J. Tyler, H.F. Arlinghaus, I. Krossing, U. Würfel, F. Glorius, *Chemistry — Eur. J.*, **29** (60), e202301482 (2023). DOI: 10.1002/chem.202301482
- [8] L. Dong, G. Zhu, H. Xu, X. Jiang, X. Zhang, Y. Zhao, D. Yan, L. Yuan, A. Yu, *Materials*, **12** (6), 958 (2019). DOI: 10.3390/ma12060958
- [9] B. Zhao, M. Nisula, A. Dhara, L. Henderick, F. Mattelaer, J. Dendooven, C. Detavernier, *Adv. Mater. Interfaces*, **7** (23), 2001022 (2021). DOI: 10.1002/admi.202001022
- [10] H. Cheng, L. Wang, R. Xiao, J. Wang, *Optik*, **262**, 169289 (2022). DOI: 10.1016/j.ijleo.2022.169289
- [11] N.V. Kamanina, P.Ya. Vasiliev, *Liquid crystal spatio-temporal light modulator based on fullerene-containing pyridine structures with orienting coatings based on carbon nanotubes*, patent RU 2 341 818 C2 (priority of 22.12.2006).
- [12] N. Kamanina, A. Toikka, D. Kvashnin, *J. Compos. Sci.*, **6** (6), 181 (2022). DOI: 10.3390/jcs6060181
- [13] N. Kamanina, A. Toikka, B. Valeev, D. Kvashnin, *J. Carbon Res.*, **7** (4), 84 (2021). DOI: 10.3390/c7040084
- [14] A.M. Bonch-Bruevich, M.N. Libenson, V.S. Makin, V.V. Trubaev, *Opt. Eng.*, **31** (4), 718 (1992). DOI: 10.1117/12.56133
- [15] R.J. Good, *J. Adhesion Sci. Technol.*, **6** (12), 1269 (1992). DOI: 10.1163/156856192X00629
- [16] S. Elmas, S. Korkmaz, S. Pat, *J. Mater. Sci.: Mater. Electron.*, **30** (9), 8876 (2019). DOI: 10.1007/s10854-019-01215-1
- [17] M. Xue, N. Peng, C. Li, J. Ou, F. Wang, W. Li, *Appl. Surf. Sci.*, **329**, 11 (2015). DOI: 10.1016/j.apsusc.2014.12.145

Translated by Ego Translating